# Airborne detection of southern pine beetle damage using key spectral bands

**Gregory A. Carter, Michael R. Seal, and Tim Haley**

**Abstract:** Damage by the southern pine beetle (SPB) (*Dendroctonus frontalis* Zimm.) occurs frequently in the southeastern United States and can result in tree death over large areas. A new technique for detection of SPB activity was tested for shortleaf pine (*Pinus echinata* Mill.) in the Caney Creek Wilderness, Ouachita National Forest, Arkansas. Digital images with 1-m pixel resolution were acquired from a light aircraft in 6- to 10-nm bandwidths centered at wavelengths of 675, 698, and 840 nm. The 675-nm band was selected to yield a maximum contrast between yellow or brown versus green foliage. The 698-nm band was selected based on its high sensitivity to leaf chlorophyll content to enable detection of less severe chlorosis in more recently damaged trees. The 840-nm band was used as a reference band that is not sensitive to chlorophyll. Images acquired within each band were calibrated to percent reflectance based on the known reflectances of a gray scale placard located on the ground. Individual trees with yellow to brown foliage were easily located in the 675- and 698-nm images. Milder chlorosis in more recently damaged pines was detected by a normalized difference vegetation index (NDVI) that was derived from 698- and 840-nm reflectances. Although statistically significant, the contrast of recently infested trees versus undamaged trees was generally visually poor in NDVI or color composite images. This was apparently a result of the inherent variability in leaf chlorophyll content throughout the forest. The increased reflectance near 700 nm characteristic of recent damage likely would be resolved more easily in pine plantations of low species diversity. Images of a NDVI that was based on 675- and 840-nm reflectances produced the strongest contrast between heavily damaged and undamaged trees.

**Résumé** : Les dommages causés par le dendroctone méridional du pin (*Dendroctonus frontalis* Zimm.) surviennent fréquemment dans le sud-est des États-Unis et peuvent entraîner la mort des arbres sur de grandes superficies. Une nouvelle technique de détection des activités de cet insecte a été testée pour le pin jaune (*Pinus echinata* Mill.) à Caney Creek Wilderness, dans la forêt nationale Ouachita, en Arkansas. Des images numériques d'une résolution de 1 m par point image ont été obtenues à partir d'un avion léger dans des largeurs de bande variant entre 6 et 10 nm, centrées sur des longueurs d'ondes de 675, 698 et 840 nm. La bande de 675 nm a été choisie pour offrir un contraste maximum entre le feuillage vert et le feuillage jaune ou brun. La bande de 698 nm a été sélectionnée en vertu de sa grande sensibilité au contenu en chlorophylle des feuilles, de façon à détecter une chlorose plus légère sur les arbres récemment atteints. La bande de 840 nm a été retenue comme bande de référence insensible à la chlorophylle. Les images obtenues dans chaque bande ont été calibrées en pourcentage de réflectance basé sur la réflectance connue d'une cible de couleur grise placée au sol. Les arbres individuels à feuillage jaune à brun étaient facilement localisés dans les images de 675 et 698 nm. Une chlorose plus légère dans les arbres récemment affectés a été décelée au moyen d'un indice différentiel normalisé de végétation (IDNV) obtenu des réflectances à 698 et 840 nm. Bien que statistiquement significatif, le contraste entre des arbres sains et des arbres récemment atteints était généralement faible sur les images en couleurs combinées ou IDNV. Ceci était apparemment dû à une variabilité inhérente dans le contenu des feuilles en chlorophylle à travers la forêt. La réflectance accrue près de 700 nm, caractéristique d'un dommage récent, pourrait probablement être résolue plus facilement dans des plantations de pin avec moins de diversité en espèces. Des images d'un IDNV basé sur des réflectances à 675 et 840 nm ont fourni le contraste le plus élevé entre les arbres fortement atteints et les arbres sains.

[Traduit par la Rédaction]

Received December 17, 1997. Accepted April 23, 1998.

**G.A. Carter.**[1] National Aeuronautics and Space Administration, Earth System Science Office, Stennis Space Center, MS 39529, U.S.A. e-mail: gcarter@sscpan.ssc.nasa.gov.
**M.R. Seal.** Institute for Technology Development, Space Remote Sensing Center, Stennis Space Center, MS 39529, U.S.A. e-mail: mseal@iftd.org.
**T. Haley.** USDA Forest Service, Forest Health Protection, Pineville, LA 71360, U.S.A. e-mail: tim.haley/r8_kisatchie@fs.fed.us

[1]Author to whom all correspondence should be addressed.

## Introduction

The southern pine beetle (SPB) (*Dendroctonus frontalis* Zimm.), a species native to North America, is the most destructive insect pest of pine forests in the southeastern United States (Payne 1980). The SPB bores through outer bark to feed on and reproduce in the phloem. Trees that have been weakened by lightning (Coulson et al. 1986), flooding, drought, or other stress agents are particularly vulnerable to SPB attack (Hicks 1980). Nevertheless, even healthy, vigorous trees may succumb to a large SPB population (Payne 1980).

Aerial photographic surveys have been used for decades to detect forest damage by the SPB (e.g., Ciesla et al. 1967). However, photographic methods have not met the long-standing need for early and even previsible detection of SPB activity (Heller 1978; Heller and Ulliman 1983). Such early detection would provide forest managers with an extremely useful tool in efforts to control damage by the SPB.

Reflectance in the 695- to 705-nm spectral band can provide early and often previsible indication of plant stress (Carter et al. 1996*a*). This is a result of the high sensitivity of reflectance near 700 nm to stress-induced chlorosis (for reviews see Carter et al. 1996*a*; Gitelson and Merzlyak 1996; Lichtenthaler et al. 1996). Thus, the use of this spectral band in high spatial resolution imagery may provide early detection of SPB damage. Indeed, needle reflectance responses to SPB attack in slash pine (*Pinus elliottii* Engelm.) indicated a maximum sensitivity to early damage at 698 nm (Entcheva et al. 1996). Reflectance near 700 nm was also an indicator of damage to lodgepole pine (*Pinus contorta* Dougl.) caused by the mountain pine beetle (*Dendroctonus ponderosae* Hopkins) in British Columbia (Ahern 1988).

Conversely, reflectance in the 670- to 680-nm range changes little in the early stages of plant stress (Carter 1993) but provides a maximum contrast between severely chlorotic and healthy foliage because of the strong absorptivity of chlorophyll in this waveband (Carter et al. 1996*b*). Reflectance in the near-infrared spectrum beyond approximately 750 nm is not influenced significantly by leaf pigmentation (Gates et al. 1965). Thus, a near-infrared band can be used in band ratios to correct at least partially for optical effects that are largely wavelength-independent (Baret and Guyot 1991; Carter 1994; Carter and Miller 1994).

The purpose of this note is to evaluate the use of narrow (6–10 nm) spectral bands centered at 675, 698, and 840 nm in reflectance imagery acquired over the Caney Creek Wilderness, Ouachita National Forest, Arkansas, for the detection of SPB damage in shortleaf pine (*Pinus echinata* Miller). This forest is a mixture of coniferous and hardwood species in mountainous terrain. Furthermore, autumn color changes had begun to occur in some deciduous trees. Thus, the Caney Creek Wilderness represented a substantial challenge for the techniques described herein.

## Materials and methods

### Study site and general approach

In late summer 1996, SPB activity was detected by the U.S. Forest Service in the Caney Creek Wilderness Area of the Ouachita National Forest in western Arkansas. On September 18, a system comprised of three digital cameras was flown over the Wilderness Area to acquire data that could be used to identify trees infested by the SPB. The flight path covered a distance of approximately 5 km, and each image frame covered a ground swath of 1.3 km. The ground area represented by each image pixel was approximately 1 × 1 m. Data were acquired in the preselected spectral bands 675 ± 5, 698 ± 3, and 840 ± 5 nm at an altitude of approximately 1830 m above ground level. These bands were selected based on general responses of leaf spectral reflectance to plant stress (Carter 1993) and needle reflectance responses to SPB damage in slash pine (Entcheva et al. 1996). Images were calibrated to percent reflectance based on the known reflectances of ground targets that were located beneath the flight path. The calibrated images then were evaluated with respect to ground observations to determine their effectiveness in detecting SPB damage.

### Airborne image acquisition

The three-camera system employed to acquire digital images of SPB sites is referred to as the Real-Time Digital Airborne Camera System (RDACS) model II, and has been described in detail (Mao and Kettler 1995). This is a second-generation system based on an earlier RDACS model I (Pearson et al. 1994). The RDACS model II is comprised of commercially available hardware, which includes three Kodak Megaplus 1.4 cameras with 12.5 mm focal length lenses and narrow bandpass (6–10 nm) interference filters, three frame grabber boards, a computer, and tape drive (Mao and Kettler 1995). The active charge-coupled device (CCD) array for each camera was comprised of 1317 pixels in the $x$ dimension and 1035 pixels in the $y$ dimension. Spectral bandpass to the CCDs was determined by the interference filters. The system was mounted in the fuselage of a piston-powered airplane (Piper Aztec). Images were acquired automatically every 8 s using a 10-ms shutter speed and were centered on a flightline of predefined GPS coordinates (Mao and Kettler 1995). Custom software was used for image storage, retrieval, and preprocessing.

### Image calibration and analysis

Data were downloaded from the onboard computer and images were band-to-band coregistered (Mao et al. 1995). Each image frame then was calibrated to percent reflectance in each of the three channels based on the known spectral reflectances of a gray-scale calibration placard that was located on the ground beneath the flight path. Because only 2 min were required to fly the 5 km path and skies were generally clear, solar irradiance changed insignificantly during data acquisition. For each band, known placard reflectance was regressed against digital gray values from the imagery to develop calibration equations. These equations then were applied to the imagery to convert digital gray values to percent reflectance.

Images of canopy reflectance in the 675-, 698-, and 840-nm bands ($R_{675}$, $R_{698}$ and $R_{840}$, respectively) were evaluated for their capability to indicate the degree of SPB damage. Pines located on SPB sites were assigned to one of three damage classes that were determined by visual observations on the ground. "Undamaged" trees had apparently not been attacked by the SPB and were characterized by dense canopies and green foliage. "Recently infested" trees also maintained dense canopies but possessed green to slightly yellow-green foliage. "Heavily damaged" or standing dead trees were characterized by yellow to reddish-brown or brown foliage and a total canopy leaf area that had been reduced to various degrees by needle abscision. Within the image of a SPB site, pixel reflectance values were sampled (ENVI version 2.6, Research Systems, Inc., Boulder, Colo.) from each of three areas that together represented all three damage classes as determined by ground observations. Each pixel was selected to represent a sunlit, 1 × 1 m

**Table 1.** Mean narrow-band reflectances and normalized difference vegetation indices (NDVI) and error and site mean squares for three active SPB sites in the Caney Creek Wilderness.

| Variable | Site 1 | Site 2 | Site 3 | EMS | SMS | $P > F$ |
|---|---|---|---|---|---|---|
| $R_{675}$ | 3.5*a* | 4.9*a* | 3.6*a* | 1.0 | 1.9 | 0.269 |
| $R_{698}$ | 8.1*a* | 10.9*a* | 8.8*a* | 1.0 | 6.1 | 0.060 |
| $R_{840}$ | 18.1*b* | 38.5*a* | 28.1*ab* | 22.8 | 312.1 | 0.016 |
| NDVI (698, 675) | 0.55*a* | 0.47*a* | 0.48*a* | 0.004 | 0.006 | 0.369 |
| NDVI (840, 675) | 0.71*a* | 0.76*a* | 0.75*a* | 0.005 | 0.003 | 0.609 |
| NDVI (840, 698) | 0.39*b* | 0.55*a* | 0.50*a* | 0.001 | 0.021 | 0.006 |

**Note:** Means were computed from values sampled for 10 trees located within each of the 3 damage classes in each of the 3 active SPB sites shown in Figs. 1 and 2 ($n$ = 30). Mean values for each damage class within a site were used in a two-way analysis of variance (ANOVA) to determine significant effects of SPB site on reflectance or a derived NDVI ($p$ = 0.05). This yielded eight total, two damage class, two site, four model, and four error degrees of freedom. Error and site mean squares (EMS and SMS, respectively) are given along with the probability of a greater value of the site $F$ statistic ($P > F$). Coefficients of determination ($r^2$) for each ANOVA ranged from 0.89 to 0.99. For a given variable (row), means followed by the same letter are not significantly different ($p$ = 0.05) as determined by Student–Neuman–Keuls test (Steel and Torrie 1960).

**Table 2.** Mean narrow-band reflectances and normalized difference vegetation indices (NDVI) and error and damage class mean squares for three SPB damage classes in the Caney Creek Wilderness.

| Variable | Undamaged | Recently infested | Heavily damaged or dead | EMS | DCMS | $P > F$ |
|---|---|---|---|---|---|---|
| $R_{675}$ | 1.3*b* | 2.3*b* | 8.4*a* | 1.0 | 45.1 | 0.002 |
| $R_{698}$ | 6.7*b* | 8.3*b* | 12.8*a* | 1.0 | 30.3 | 0.004 |
| $R_{840}$ | 32.0*a* | 30.1*a* | 22.5*a* | 22.8 | 76.1 | 0.141 |
| NDVI (698, 675) | 0.69*a* | 0.59*a* | 0.21*b* | 0.004 | 0.190 | 0.002 |
| NDVI (840, 675) | 0.92*a* | 0.85*a* | 0.44*b* | 0.005 | 0.204 | 0.002 |
| NDVI (840, 698) | 0.64*a* | 0.54*b* | 0.26*c* | 0.001 | 0.118 | <0.001 |

**Note:** Means were computed from values sampled for 10 trees located within each of the three damage classes in each of the three active SPB sites shown in Figs. 1 and 2 ($n$ = 30). Mean values for each damage class within a site were used in a two-way analysis of variance (ANOVA) to determine significant effects of SPB damage on reflectance or a derived NDVI ($p$ = 0.05). This yielded eight total, two damage class, two site, four model. and four error degrees of freedom. Error and damage class mean squares (EMS and DCMS, respectively) are given along with the probability of a greater value of the damage class $F$ statistic ($P > F$). Coefficients of determination ($r^2$) for each ANOVA ranged from 0.89 to 0.99. For a given variable (row), means followed by the same letter are not significantly different ($p$ = 0.05) as determined by Student–Neuman–Keuls test (Steel and Torrie 1960).

portion of a tree canopy, but pixels were not matched exactly with individual trees on the ground. Values were recorded for 1 pixel per each of 10 trees within each damage class and SPB site. Pixel values were recorded for all three spectral bands, as well as for various normalized difference vegetation indices (NDVI). These NDVI were effectively band ratios, and were computed as (*i*) $(R_{698} - R_{675})/(R_{698} + R_{675})$; (*ii*) $(R_{840} - R_{675})/(R_{840} + R_{675})$, or (*iii*) $(R_{840} - R_{698})/(R_{840} + R_{698})$.

The reflectance or NDVI pixel values sampled from each damage class, as described above, were used to determine statistically the effectiveness of this technique in the separation of damage classes within an image. Significant ($p$ = 0.05) SPB effects on reflectance or a NDVI, as well as among-site differences in these values, were determined by analysis of variance (ANOVA). Data were replicated equally among classes and were distributed normally within site and damage class. The Student–Newman–Keuls means comparison test (Steel and Torrie 1960) determined significant differences among damage class and site means (SAS version 6.0, SAS Institute, Cary, N.C.). Thus, a significant difference in reflectance or NDVI values among damage classes indicated that reflectance in a given waveband or a particular NDVI was successful in distinguishing the level of SPB damage. Scatterplots and color composite images were used additionally to evaluate the effectiveness of various band combinations in the detection of early damage symptoms.

## Results and discussion

Numerous SPB sites were located in the Caney Creek Wilderness, and all were detected by visual inspection of $R_{675}$, $R_{698}$, NDVI, or color composite images. Most of these sites were a result of infestations that occurred during the previous year, 1995, and thus were comprised of heavily damaged or standing dead trees that had been vacated by the SPB. Nevertheless, three of the sites contained active SPB populations and included trees that represented each of the three damage classes. The effect of location, or site, on reflectances and NDVI was generally not significant ($p$ = 0.05) (Table 1). Exceptions were a range in $R_{840}$ among sites of approximately 20% and a low NDVI (840, 698) on Site 1. These exceptions resulted from variability among sites in the degree of needle loss from heavily damaged or standing dead trees.

$R_{698}$ and $R_{675}$ distinguished between heavily damaged or

**Fig. 1.** Digital images of the normalized difference vegetation index (NDVI) computed as $(R_{840} - R_{698})/(R_{840} + R_{698})$ for three sites infested by the southern pine beetle. Image scale is indicated in Fig. 1A, and arrows identify areas surveyed by ground inspection. Pixel ground size is approximately 1 × 1 m. Linear features in the upper left corner of Fig. 1A (site 1) and progressing toward midframe are a stream, unpaved road, and power line, respectively. The stream is seen also in the upper portion of Fig. 1B (site 2). Dark areas in the lower right corner of Fig. 1C (site 3) are standing dead trees. Each image contains 640 pixels in the $x$ direction and 480 pixels in the $y$ direction.

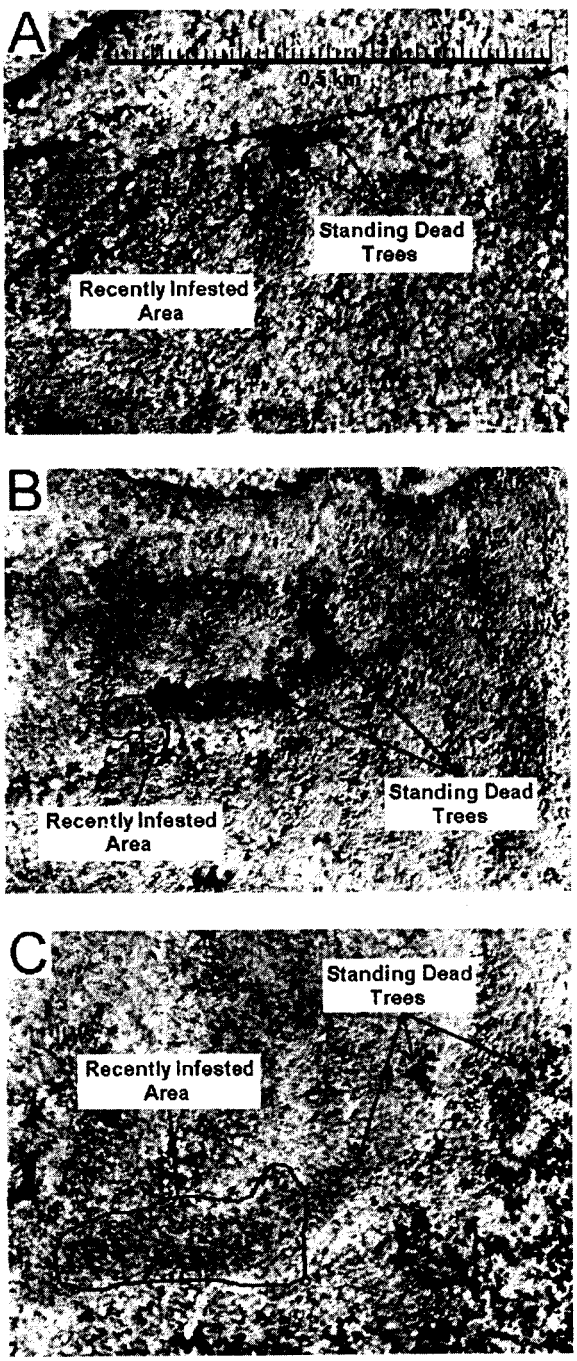


**Fig. 2.** Digital images of the normalized difference vegetation index (NDVI) computed as $(R_{840} - R_{675})/(R_{840} + R_{675})$ for three sites infested by the southern pine beetle. Image scale is indicated in Fig. 2A, and arrows identify areas surveyed by ground inspection. Pixel ground size is approximately 1 × 1 m. Linear features in the upper left corner of Fig. 2A (site 1) and progressing toward midframe are a stream, unpaved road and power line, respectively. The stream is seen also in the upper portion of Fig. 2B (site 2). Dark areas in the lower right corner of Fig. 2C (site 3) are standing dead trees. Each image contains 640 pixels in the $x$ direction and 480 pixels in the $y$ direction.

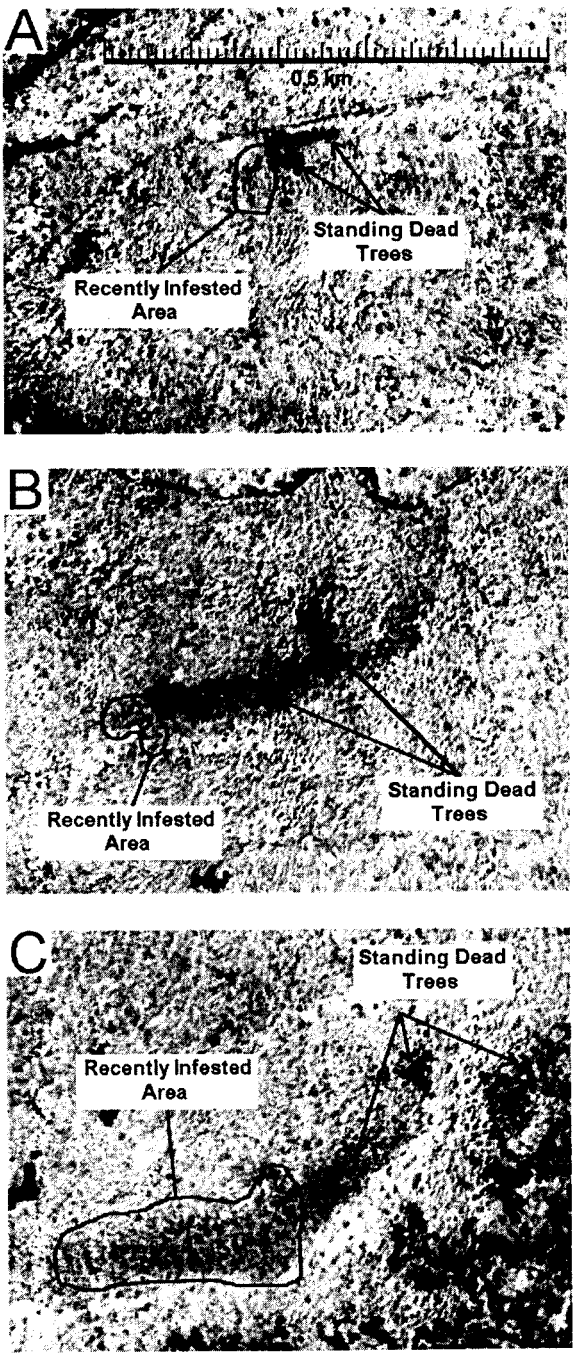


standing dead trees versus the two remaining classes (Table 2). $R_{840}$ tended to be lower in standing dead trees as a result of needle loss. Neither reflectances alone nor the NDVIs based on $R_{840}$ and $R_{675}$ (abbreviated NDVI (840, 675) or NDVI (698, 675)) could distinguish undamaged from recently infested trees. However, NDVI (840, 698) distinguished

between undamaged and recently infested trees, as well as between either of these two classes and heavily damaged or standing dead trees (Table 2). Although canopy optical density is influenced by the amount and distribution of foliage as well as leaf pigmentation, recently infested trees showed no signs of foliar wilting or loss compared with undamaged trees. Thus, differences in NDVI (840, 698) between recently infested and undamaged trees were probably a result of damage-induced differences in leaf chlorophyll content. The significant response of NDVI (840, 698) to this apparent difference is explained by its high sensitivity to the chlorophyll content in optically dense canopies (Carter 1998).

Although NDVI (840, 698) detected recently damaged areas on a statistical basis, image contrast between recently damaged trees and the surrounding forest was poor in the NDVI (840, 698) images (Fig. 1). This is most likely explained by the inherent variability in leaf chlorophyll contents throughout uninfested areas of the forest. This variability is attributed to differences in leaf chlorophyll content among undamaged pines and may have been influenced also by other species and incipient autumn senescence in deciduous trees. The NDVI images based on $R_{698}$ and $R_{675}$ were similar in general appearance to Fig. 1 and thus are not shown.

NDVI (840, 675) yielded the greatest contrast between heavily damaged or dead trees and surrounding undamaged trees (Fig. 2). This high contrast is explained primarily by the strong absorptivity of chlorophyll at wavelengths near 675 nm, as discussed earlier (Carter et al. 1996*b*). Thus, green to slightly chlorotic foliage contrasts strongly with yellow to brown foliage in the NDVI (840, 675) images.

Similar to ANOVA results, scatterplots indicated that all two-band combinations distinguished between heavily damaged or standing dead trees and the remaining two classes (Fig. 3). The $R_{698}$ and $R_{840}$ band combination yielded the strongest separation of undamaged and recently infested trees. Nevertheless, false color composite images of each site provided no clearer separation among damage classes than the NDVI images and thus are not shown.

## Conclusions

Individual trees with yellow to brown foliage and classified as heavily damaged by the SPB were easily located in 675- and 698-nm reflectance images. Statistically, mild chlorosis in recently infested pines was detected by a NDVI derived from 840- and 698-nm imagery. However, this was not easily resolved visually in the NDVI images. Results were similar for false-color composite images. This result was explained by an apparent variability in leaf chlorophyll contents among undamaged pines and may have been influenced also by the diverse species mixture and incipient autumn color changes in deciduous trees. A NDVI derived from 840- and 675-nm reflectances provided the strongest contrast of heavily damaged or standing dead trees versus undamaged trees and, thus, was the most effective image for location of SPB-damaged sites. Detection of recent damage using the present technique depends entirely on the capability to detect small decreases in leaf chlorophyll contents. Thus, it is expected that the increased reflectance near 700 nm characteristic of early damage-induced chlorosis would be resolved more easily in pine plantations because of their characteristically even age and lower species diversity.

**Fig. 3.** Relationships among canopy reflectances in the 675-, 698-, and 840-nm wavebands. These scatterplots indicate the effectiveness of various band combinations in distinguishing among undamaged (○), recently infested (□) and heavily damaged or standing dead (△) trees. Open symbols represent pixel (1 × 1 m) reflectance values for sunlit portions of 10 trees per damage class sampled from each of three SPB sites. Closed symbols (●, undamaged; ■, recently infested; ▲, heavily damaged or dead standing) represent the mean values for each damage class as listed in Table 2. Note different scales among graphs. The strongest segregation between values for undamaged (○) and recently infested (□) trees occurs in Fig. 3C.

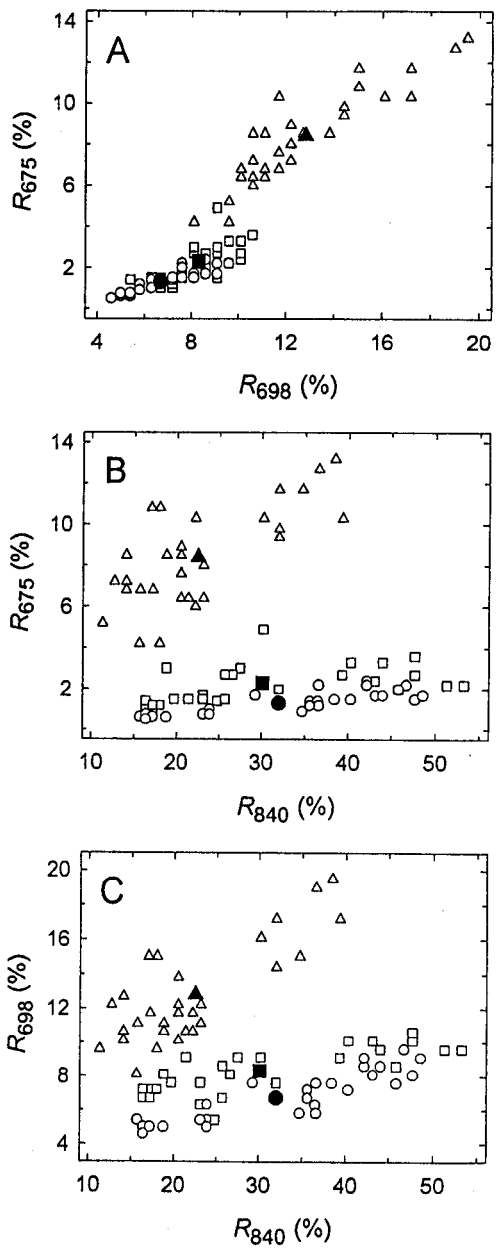

## Acknowledgements

This project was supported by a grant from the USDA Forest Service, Southern Global Change Program. Thanks to Jim Anderson for assistance with preparation of the figures.

## References

Ahern, F.J. 1988. The effects of bark beetle stress on the foliar spectral reflectance of lodgepole pine. Int. J. Remote Sens. **9**: 1451–1468.

Baret, F., and Guyot, G. 1991. Potentials and limits of vegetation indices for LAI and APAR assessment. Remote Sens. Environ. **35**: 161–173.

Carter, G.A. 1993. Responses of leaf spectral reflectance to plant stress. Am. J. Bot. **80**: 239–243.

Carter, G.A. 1994. Ratios of leaf reflectances in narrow wavebands as indicators of plant stress. Int. J. Remote Sens. **15**: 697–703.

Carter, G.A. 1998. Reflectance wavebands and indices for remote estimation of photosynthesis and stomatal conductance in pine canopies. Remote Sens. Environ. **63**: 61–72.

Carter, G.A., and Miller, R.L. 1994. Early detection of plant stress by digital imaging within narrow stress-sensitive wavebands. Remote Sens. Environ. **50**: 295–302.

Carter, G.A., Cibula, W.G., and Miller, R.L. 1996*a*. Narrow-band reflectance imagery compared with thermal imagery for early detection of plant stress. J. Plant Physiol. **148**: 515–522.

Carter, G.A., Dell, T.R., and Cibula, W.G. 1996*b*. Spectral reflectance characteristics and digital imagery of a pine needle blight in the southeastern United States. Can. J. For. Res. **26**: 402–407.

Ciesla, W.M., Bell, J.C., Jr., and Curlin, J.W. 1967. Color photos and the southern pine beetle. Photogramm. Eng. **33**: 883–889.

Coulson, R.N., Flamm, R.O., Pulley, P.E., Payne, T.L., Rykiel, E.J., and Wagner, T.L. 1986. Response of the southern pine bark beetle guild (Coleoptera: Scolytidae) to host disturbance. Environ. Entomol. **15**: 850–858.

Entcheva, P.K., Cibula, W.G., and Carter, G.A. 1996. Spectral reflectance characteristics and remote sensing detection of southern pine beetle infestation. *In* Proceedings of the Eco-Informa Conference, 4–7 November, 1996, Lake Buena Vista, Florida. Environmental Research Institute of Michigan, Ann Arbor, MI, Tech. Program Abstr. F-12.

Gates, D.M., Keegan, H.J., Schleter, J.C., and Weidner, V.R. 1965. Spectral properties of plants. Appl. Optics **4**: 11–20.

Gitelson, A.A., and Merzlyak, M.N. 1996. Signature analysis of leaf reflectance spectra: algorithm development for remote sensing of chlorophyll. J. Plant Physiol. **148**: 494–500.

Heller, R.C. 1978. Case applications of remote sensing for vegetation damage assessment. Photogramm. Eng. Remote Sens. **44**: 1159–1166.

Heller, R.C., and Ulliman, J.J. (*Editors.*) 1983. Forest resource assessments *In* Manual of remote sensing. 2nd ed. Vol. 2. *Edited by* J.E. Estes and G.A. Thorley. American Society for Photogrammetry, Falls Church, Va. pp. 2229–2324.

Hicks, R.R., Jr. 1980. Climatic, site and stand factors. *In* The southern pine beetle. USDA For. Serv. Sci. Educ. Admin. Tech. Bull. No. 1631. pp. 55–68.

Lichtenthaler, H.K., Gitelson, A., and Lang, M. 1996. Non-destructive determination of chlorophyll content of leaves of a green and an Aurea mutant of tobacco by reflectance measurements. J. Plant Physiol. **148**: 483–493.

Mao, C., and Kettler, D. 1995. Digital CCD cameras for airborne remote sensing. *In* Proceedings, 15th Biennial Workshop on Videography and Color Photography in Resource Assessment, 1–3 May, 1995, Terre Haute, Ind. American Society of Photogrammetry and Remote Sensing, Bethesda, MD. pp. 1–12.

Mao, C., Howard, S., and Grace, J. 1995. Pre-processing of airborne digital CCD camera image. Proceedings, 15th Biennial Workshop on Videography and Color Photography in Resource Assessment, 1–3 May 1995, Terre Haute, Ind. American Society of Photogrammetry and Remote Sensing, Bethesda, MD. pp. 106–114.

Payne, T.L. 1980. Life history and habits. *In* The southern pine beetle. USDA For. Serv. Sci. Educ. Admin. Tech. Bull. No. 1631. pp. 7–28.

Pearson, R., Grace, J., and May, G. 1994. Real-time airborne agricultural monitoring. Remote Sens. Environ. **49**: 304–310.

Steel, R.G.D., and Torrie, J.H. 1960. Principles and procedures of statistics. McGraw-Hill, New York.